Effect of Nucleotide Binding on Rad50 Conformational State, Multimeric State, and DNA Binding Ability

Eric Estrin

Honors Thesis Spring 2009

Dean's Scholars Honors Program

Department of Chemistry and Biochemistry

The University of Texas at Austin

May 7, 2009

_____

Tanya T. Paull, Ph.D.

Molecular Genetics and Microbiology

Supervising Professor

_____

Adrian Keatinge-Clay, Ph.D.

Chemistry and Biochemistry

Second Reader

Contents

Contents……2

Abstract……...……..3

Introduction……...……4

Materials and Methods……11

Results.……17

Discussion……..…..32

References……..……..37

Acknowledgements…….…….42

Abstract

The ability of an organism to swiftly repair double-stranded breaks (DSBs) in DNA is a crucial process that, if absent, can result in genomic instability. The Mre11/Rad50 protein complex is highly conserved and plays a key role in sensing, processing, and repairing DNA DSBs. Rad50 is known to be necessary for the DNA end-bridging catalyzed by the MRN complex, and association of the broken DNA ends is essential to prevent loss of chromosome fragments *in vivo*. The Rad50 protein contains a large coiled-coil domain and ATP-binding motifs, with an overall structure similar to the Structural Maintenance of Chromosomes (SMC) family of proteins. Rad50 undergoes ATP-dependent homodimerization, which creates a potential DNA binding cleft. Recently, Rad50 has been shown to have adenylate kinase activity in addition to the previously known ATPase activity. It is still unknown what role ATP-induced dimerization and conformational changes play in pfRad50's various activities. We hypothesize that dimerization is needed for DNA binding, and that Rad50 requires large conformational changes for proper function in its part in pfMR exonuclease activity. Here, we use site-directed mutagenesis to create Rad50 mutants that have cysteines placed in structurally relevant portions of the protein. With these cysteines, we used disulfide crosslinking, fluorescence, and Fluorescence Resonance Energy Transfer (FRET) to detect if changes in conformation or multimeric state of Rad50 are necessary for adenylate kinase activity, ATPase activity, and DNA binding.

Introduction

In all forms of life, the ability to maintain the integrity of chromosomal DNA is necessary for cells to survive. While the importance of DNA repair has been highlighted recently due to its relationship to cancer and other diseases, the study of genetic repair didn't develop as rapidly as other fields of genetic function. This situation emerged in large part due to the prevailing thought in the 1930s that protein, which was thought to be fundamentally quite stable, was the main genetic information in life. Additionally, cell recovery after significant radiation was poorly documented. However, in the early 1940s, both the Demerec and Luria labs discovered enzymatic photoreactivation, wherein bacteria exposed to UV radiation would recover if after irradiation the cells were exposed to visible light. This was the first proof of a DNA repair mechanism, and many other mechanisms were found for different types of DNA damage. As molecular biology flourished, it became clear that each type of radiation caused a different type of DNA lesion, which was repaired by a separate process. Double-strand breaks (DSBs) are now documented as one of the most cytotoxic types of DNA damage.(Stewart et al., 1999) These breaks are characterized by two simultaneous DNA nicks (that is, breaks in the sugar-phosphate backbone of DNA) on opposite sides of a DNA helix. If these nicks must occur within a close distance to each other, such that the chromatin structure and base-pairing of the two DNA ends do not permit their juxtaposition, then the DNA helix is severed.

DSBs are introduced into cells from environmental insults, such as ionizing radiation, topoisomerase inhibitors, and radiomimetic drugs, as well as from intermediates in normal physiological processes. (Karagiannis and El-Osta, 2004) One well-documented case of

intentionally introduced DSB formation is that of the Spo11 endonuclease, which catalyzes DSBs during meiotic recombination. Additionally, in V(D)J recombination, DSBs are introduced by the RAG1/RAG2 nuclease complex in the process of creating diversity amongst immunoglobin heavy and light chain variable regions in lymophyctes. (Gellert, 2002) An unrepaired DSB can arrest or kill a cell, while a misrepaired DSB can result in cancer.

Not surprisingly, then, cells have evolved robust mechanisms for managing and repairing DSBs. In eukaryotes, two alternative repair pathways have developed for DSBs: homologous recombination (HR) and nonhomologous end joining (NHEJ). (Chen and Kolodner, 1999) In homologous recombination, sister chromatids (or homologous chromosomes, during meiotic recombination) are used as templates for repair without loss of genetic information. At the first step of HR, 3' single-stranded tails are produced by an exonuclease that resects the open 5' DNA ends. Then, a recombinase, such as RecA in prokaryotes or Rad51 in eukaryotes, binds to these 3' tails. This nucleoprotein complex then catalyzes single-strand invasion of the opposite, homologous region of the sister chromatid (or homologous chromosome). This 3' invading end displaces the complementary chromatid strand and DNA synthesis is primed. Meanwhile, the other end of the double strand break anneals to the displaced complementary strand and a structure known as a Holliday junction is formed. DNA is synthesized using the intact complementary strands and the templates are unwound and allowed to anneal. Finally, any remaining DNA nicks are sealed by a ligase. Homologous recombination is the major pathway of DSB repair in prokaryotes and lower eukaryotes, but primarily occurs during the G2 and S phases of the cell cycle, when sister chromatids are present.

Alternatively, DSBs can be repaired by non-homologous end-joining (NHEJ). In NHEJ, the two broken ends are directly ligated, sometimes guided by microhomologies between the two

ends. (Lewis and Resnick, 2000), (Weterings and van Gent, 2004) Processing of damaged DNA ends through this pathway often results in a loss of DNA sequence at the breakpoints. In mammalian cells, the most likely determinant of which pathway is chosen is cell-cycle stage, with NHEJ strongly favored in G1. (Takata et al., 1998)

When looking for genes involved in double-strand break repair in yeast, researchers used screens to find mutants that were sensitive to radiation or had defects in meiotic recombination. (Ajimura et al., 1993; Ivanov et al., 1992; Kupiec and Simchen, 1984) Genes that when mutated displayed these phenotypes, were labeled as Rad (*Rad*iation sensitivity), Xrs (*x-r*ay *s*ensitivity), or Mre (*m*eiotic *re*combination). This screen led to the discovery of three genes, Mre11, Rad50, and Xrs2, which form a multiprotein complex, termed the MR(N/X) complex. Each component showed similar phenotypes when mutated and subjected to radiation. Mre11 and Rad50 genes were found to be highly conserved in evolution and shown to be analogous to the SbcC and SbcD genes found in *E.* coli.(Aravind et al., 1999; Blinov et al., 1989; Gorbalenya and Koonin, 1990) Using a two-hybrid screen, Rad50 and Mre11 were shown to physically interact in yeast.(Johzuka and Ogawa, 1995) There wasn't as much success when trying to identify functional homologs of the third component, Xrs2, of this epistasis group; however, Nbs1 was shown to copurify with Mre11 and Rad50 in humans, and shows limited homology to Xrs2.(Carney et al., 1998)

The MRN complex has been shown to harbor many different cellular functions, all related to double strand break metabolism. In humans, hypomorphic mutations in Nbs1 and Mre11 cause Nijmegen breakage syndrome and Ataxia Telangiectasia Like Disease, respectively, which both result in chromosomal instability and cancer predisposition. These symptoms are similar to those found in the well-studied Ataxia-Telangiectasia disease, which is

caused by mutations in ATM, a serine/threonine specific protein kinase that activates pathways for cell cycle checkpoint control in eukaryotic cells.(Shiloh, 2003) ATM exists as an inactive dimer in the nucleus, and after DNA damage is known to become a monomer, which is the active state.(Bakkenist and Kastan, 2003) This activated monomer has been shown to adhere to chromatin and to phosphorylate, among other cell cycle regulators, the tumor suppressor p53. The MRN complex was shown to be required for ATM activation, which led researchers to believe that MRN is a DNA damage sensor.(Goldberg et al., 2003; Stewart et al., 2003)

Additionally, yeast Spo11, the endonuclease involved in meiotic recombination mentioned earlier, requires the presence of the MRN complex to create double strand breaks.(Alani et al., 1990) The MRN complex has been shown to repair damaged DNA caused by chemical and physical sources, to associate with replication origins during S phase, and promotes sister-chromatid recombination. including hairpin DNA. (Maser et al., 2001; Mirzoeva and Petrini, 2003)

It is also believed that Rad50 may mediate the physical connection between two pieces of DNA, such as that needed when ligating two pieces of DNA during NHEJ or joining sister chromatids during HR. This theory is supported by the finding that MRX is required for tethering of DSBs *in vivo*.(Kaye et al., 2004) Thus, it is thought that the MRN complex acts to increase the local concentration of DSBs. Electron microscopy and scanning force images have created images of the MRN complex with a head region and two long tails.(Chamankhah et al., 2000; de Jager et al., 2001) This architecture suggests many possibilities of physically linking two separated pieces of DNA, such as by forming a ring-like structure around one piece of DNA, with the head segment binding a second piece of DNA, or with two MRN complexes interacting through the end of the tail regions while each head region binds DNA. (Hopfner et al., 2001)

Biochemical characterization of Rad50 and Mre11 showed that Rad50 is an ATPase with a large coiled-coil domain, while Mre11's N-terminal domain contains a putative phosphodiesterase domain that is responsible for its phosphatase with dsDNA 3', 5' exonuclease and ssDNA endonuclease activities. This N-terminal domain also contains a Nbs1/Xrs2 interaction site. (Hopfner, 2006) The nuclease activity of Mre11 is thought to be involved in cleaning up misfolded DNA ends that occur at DNA breaks. (Lobachev et al., 2002) After removal of damaged DNA ends, DNA polymerases could then efficiently extend the 3' end to form a repaired DNA molecule. Additionally, the nuclease activity of Mre11 has been shown to be necessary for the efficient removal of covalently bound Spo11 from the 5' end of meiotic DSBs.(Hopfner et al., 2000)

Mre11 also has a C-terminal DNA-binding/active capping site domain that, based on structural data, has the proper surface for binding ssDNA. Additionally, this domain is likely to contain Rad50 interaction and Mre11 dimerization motifs. Due to its ability to bind both Nbs1/Xrs2 and Rad50, as well as dimerize with itself, it is believed that Mre11 forms the architectural core of the MRN complex.

Unique to eukaryotes is the presence of Nbs1/Xrs2 in the MRN complex. The least well understood of the three components of the complex, Nbs1/Xrs2 contains an N-terminal *f*ork*h*ead associated domain (FHA) along with a C-terminal breast cancer associated domain. This component binds to ATM, Mdc1, and other phosphorylated proteins and thus is important in localizing the complex to sites of DNA breaks. (Lukas et al, 2004) However, as a Xrs2/Nbs1 homolog hasn't been found in archaea or bacteria, this component is likely to be involved in eukaryotic-specific functions such as cell cycle control or sexual reproduction.

Rad50 is an ATPase that is related to the *A*TP *b*inding *c*assette (ABC) transporter family of proteins. It should be noted that although Rad50 is related to the ABC transporter family of proteins, it is itself not one, as it does not contain the ABC transporters are transmembrane proteins that are functionally diverse, but generally work in moving chemicals across cell membranes. They are found in organisms from all kingdoms, and make up 2% of the *E. coli* genome. (Moreau et al., 1999) There are 48 currently known in the human genome and these have been implicated to be involved in the molecular resistance to cancer and pathogenic microbe's resistance to drugs. (Linton and Higgins, 1998) They contain a modular architecture, marked by two nucleotide binding domains (NBDs) and two transmembrane domains (TMDs). Notably, the structure of the Rad50 catalytic domains published in 2000 was the second high-resolution crystal structure of an ABC catalytic domain, and remains one of the most well studied ABC transporter-like proteins.(Klein et al., 1999) Thus, any work done to elucidate the mechanism and function of Rad50 has implications towards ABC transporters.

Rad50's ATPase activity arises from Walker A and Walker B motifs found at either end of the two catalytic domains of Rad50 and a C-terminal loop, called the 'signature motif'. Rad50's ATP binding capability has been shown to be necessary in all activities of the MRN complex in yeast. (Hopfner et al, 2001) Binding stimulates homodimerization of Rad50 catalytic domains, which enables Rad50's ability to melt DNA structures, process hairpins, and increase its own DNA binding ability.(de Jager et al., 2002; Paull and Gellert, 1998; Trujillo and Sung, 2001; Zhang and Paull, 2005) Rad50 was also shown to possess both forward and reverse adenylate kinase activity, the forward reaction being a transfer of phosphate from ATP to AMP to yield two ADP molecules.(Bhaskara et al., 2007) Thus, there are at least a few different nucleotide bound states of Rad50, such as two ADP molecules bound, two ATP molecules

bound, or an ATP and an AMP molecule, or no nucleotides bound. It is likely that these different nucleotide bound states correspond to functionally different conformations/multimerizations of Rad50, and would thus act as a kind of switch. It is unclear, however, of the role ATP hydrolysis plays in Rad50's activity in the cell, but may be a way for Rad50 to exit its ATP bound, homodimerized state.

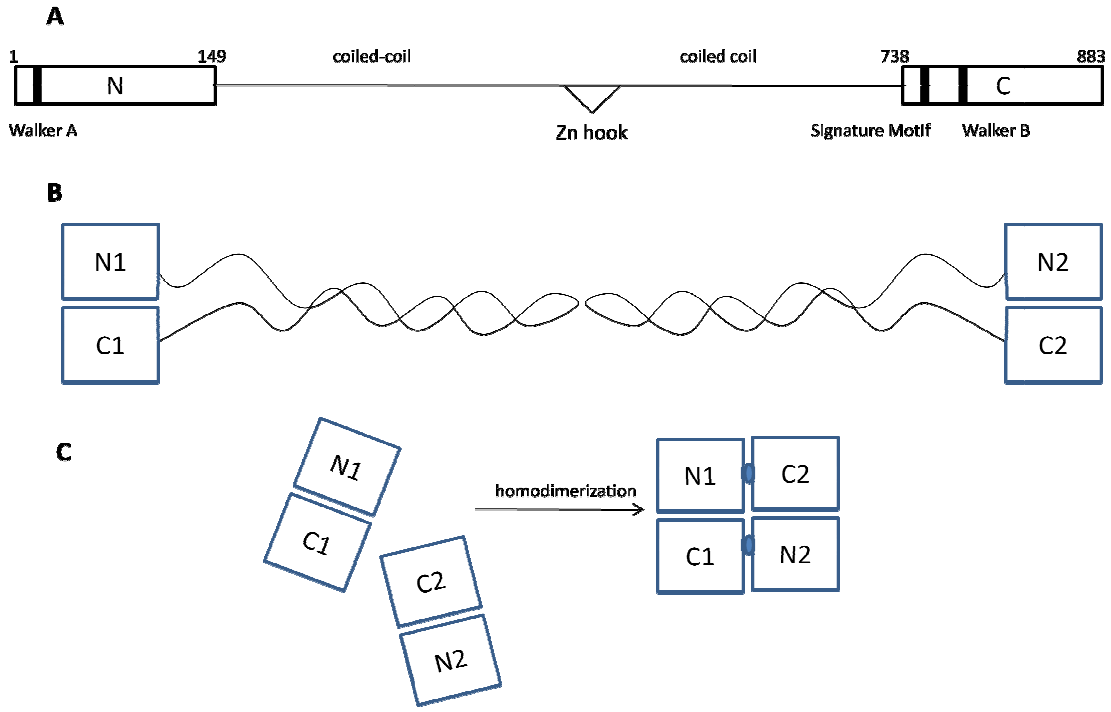

Figure 1: Idealized structure and dimerization of Rad50. (A) Gene structure of Rad50. (B) Structure of full length, non-dimerized Rad50. (C) Top view of Rad50 catalytic domain dimerization. ATP is labeled as blue ovals.

In this work, I have attempted to understand the ATP-dependent structural changes necessary for *Pyrococcus furiosus* Rad50 (pfRad50) function. It is still unknown what role ATP-induced dimerization and conformational changes play in pfRad50's various activities. We hypothesize that dimerization is needed for DNA binding, and that Rad50 requires large conformational changes for proper function in its part in pfMR exonuclease activity. I have used a combination of biochemical techniques, including DNA exonuclease assays, Fluorescence

Resonance Energy Transfer (FRET), and site-directed crosslinking to address these questions *in vitro*.

Methods and Materials

Construct and mutagenesis

pfRad50-SMA plasmid and pfMR was given as a gift to Tanya Paull by John Tainer and Karl-Peter Hopfner. The SMA construct contained the N and C terminal domains of the *Pyrococcus furiosus* Rad50 gene only (that is, without the coiled coil domains). The pfMR construct consists of the full length Rad50 and Mre11 genes, controlled by the same promoter to enable coexpression. The plasmids also contains a gene for kanamycin antibiotic resistance which was used as a selectable marker to select for bacteria that received the plasmid during transformation. This plasmid was modified by site-directed mutagenesis using the Quikchange method according to the manufacturer's instructions (Stratagene).

Transformation

Ultracompetent XL-10 Gold cells (Stratagene) were transformed with the Quickchange mutated SMA-pfRad50 or pfMR plasmid. 45 uL of cells were incubated on ice with 2 uL B-mercaptoethanol for 10 min. Then, 3 uL of Quickchange plasmid was added and this was incubated for an additional 30 minutes on ice. Cells were then heatshocked for 45 seconds at 42°C and allowed to recover for two minutes on ice. Cells were then grown in at 37°C shaking at approximately 220 rpm for 45 minutes after 300 uL Luria Broth was added. The cells were then plated on Luria Broth + kanamycin plates and grown at 37°C overnight. These cells were then miniprepped and sequenced to make sure they had the appropriate plasmid and mutation(s). The plasmids were then transformed into competent *E. coli* BL21DE for expression. This was done

using the same protocol as for the XL-10 Gold cells, except B-mercaptoethanol wasn't added and 1 uL of plasmid was incubated on ice with 10 uL of competent cells. The resulting colonies were then grown in Luria Broth overnight at 37°C and, 900 uL of this was mixed with 100 uL Dimethyl sulfoxide (DMSO) (added as a cryoprotectant) and stored at -80°C.

Induction

The following methods were adapted from Hopfner *et al.* 2000. A single colony of BL21DE *E.coli* cells was used to inoculate 100 ml of Luria broth containing kanamycin, (50 µg/ml) and this culture was grown overnight at 37°C with shaking. Then all 100 ml of this overnight culture was used to seed 1 L of Luria broth containing kanamycin (50 µg/ml), and cells were grown at 37°C with shaking to an optical density at 600 nm of 1.0. Protein expression was induced by adding isopropyl-beta -D-thiogalactopyranoside (IPTG) to a final concentration of 0.8 mM, and the culture was incubated for longer. After 3.5 hours, the cells were harvested by centrifugation and, if necessary, frozen in liquid nitrogen.

Purification

pfRad50-SMA and full length pfMR proteins were isolated by resuspending the cells in 20 ml of a mixture containing 50 mM sodium phosphate (pH 8.0), 50 mM KCl, 2.5 mM imidazole, 10% glycerol, 20 mM BME, 1mM PMSF, and 0.5% Tween. Cells were disrupted using a French Press. Cells were additionally disrupted by sonication, and insoluble matter was pelleted by centrifugation at 100,000 × g (35,000 RPM), using a 70Ti rotor in a Beckman Optima LE-80K Ultracentrifuge (complements of the Lambowitz lab). As the SMA protein is heat stable, the supernatant was heat shocked at 75°C for 10 min to precipitate all non-heat stable proteins. Precipitated protein was removed by centrifugation at 30,000 × g using a Beckman

Coulter Avant J-20 centrifuge. The supernatant from this step was loaded on 5 ml of Ni2+-nitrilotriacetic acid (Ni-NTA) resin (Qiagen), and the column was washed with 50 ml Nickel A buffer containing 50 mM phosphate (pH 8.0)-500 mM NaCl-2.5 mM imidazole, 10% glycerol followed by 50 ml of Nickel A buffer containing 200 mM NaCl. Bound protein was eluted with a linear gradient of 2.5 to 250 mM imidazole in Nickel A buffer containing 250 mM NaCl. Fractions from this column were assayed by sodium dodecyl sulfate-polyacrylamide gel electrophoresis (SDS-PAGE) and Coomassie blue staining; pfRad50 eluted from this column between 100 mM and 160 mM imidazole-10% glycerol. Approximately 10 mL of the pfRad50-containing fractions were pooled and loaded onto a 1mL Hi-trap Q anion-exchange column. The column was washed with 50 ml of buffer A contaninig 100 mM NaCl, 25mM Tris pH 8, 10% glycerol, and 1 mM DTT, and the protein was eluted with buffer A containing 600 mM NaCl. The peak fractions from this elution, assayed by SDS-PAGE and Coomassie blue staining as described earlier were pooled and subjected to further purification using a SP cation-exchange column. The pooled peak fractions were diluted 1X using 100mM NaCl, 25mM Tris pH 8, 10% glycerol, and 1mM DTT to allow the protein to bind to the column. After loading, the column was washed using 100mM NaCl, 25mM Tris pH 8, 10% glycerol and eluted using a step to 600 mM NaCl salt. 500 uL fractions were taken. For SMA-pfRad50 samples, the peak fractions were aliquoted into 15 uL fractions and frozen in liquid nitrogen. For pfMR samples, the peak fractions from this elution, assayed by SDS-PAGE and Coomassie blue staining as described earlier were pooled and subjected to further purification using a Superose 200 gel filtration column. Proteins were injected on to a Superose 200 column and separated in 50 mM Tris (pH 8.0)-100 mM NaCl-1 mM dithiothreitol (DTT)-10% glycerol at a flow rate of .4mL/min. As

assayed by SDS-PAGE and Coomassie blue staining, the fraction with the highest concentration of pfMR was aliquoted into 15 μL fractions and frozen in liquid nitrogen.[10]

Protein Quantification

Protein quantification was carried out by running a titration of a known concentration of BSA on an SDS-PAGE gel and titration of protein, stained with Coomassie blue. This gel was then scanned using a Licor Odyssey scanner and the image quantified using ImageQuant 5.1 software (Molecular Dynamics). A calibration curve was created and only the linear area of the plot used.

TLC ATPase and adenylate kinase assays

For ATPase and adenlyate kinase assays, pfRad50 was incubated in 10 μl reactions containing buffer A (20 mM Tris [pH 8.0], 100 mM NaCl, 10% glycerol, 1 mM DTT) with 5 mM $MgCl_2$, 500 uM cold AMP, 2 mM DTT, and 50 μM [γ-^{32}P]ATP. Reactions were incubated at 65°C for one hour and were stopped with the addition of 1% SDS and 10 mM EDTA. The reaction (1 μl) was then spotted on a polyethyleneimide (PEI) plate (EMD Biosciences) and separated by thin layer chromatography (TLC) for ATP, ADP, and P_i using 0.75 M KH_2PO_4 (pH 3.4). The plates were dried and analyzed by phosphorimager (Bio-Rad). The levels of P_i generated were used as a measure of ATPase activity, and the levels of [β-^{32}P]ADP were used as a measure of adenylate kinase activity.

Crosslinking assays

Intradimer and interdimer crosslinking ability of mutant proteins was assessed using SDS-PAGE, as disulfide bonds present in the proteins would not be disrupted if run in buffer that

contained reducing agent. Intradimer crosslinking was assessed by incubating purified protein with varying amounts of hydrogen peroxide, a strong oxidizing agent for five minutes on ice. SDS loading buffer with and without B-mercaptoethanol, a strong reducing agent, was then added and the resulting solution was boiled for 10 minutes to denature the protein.

Interdimer crosslinking was assessed using three steps. Initially, DTT was added to the protein and incubated for five minutes on ice, after which 5mM $MgCl_2$ and .5 mM ATP were added and the mixture was incubated for ten minutes at 65°C. Finally, an excess (2mM) H_2O_2 or 300 nM diamide was added and this allowed to incubate for 5 minutes on ice. The resulting mix was then run on a SDS-PAGE gel with or without reducing agent in the loading buffer as indicated

Cy3/Cy5 Maleimide dye conjugation

Protein was diluted to 1mg/mL concentration using 500mM NaCl, 25mM Tris pH 8, 10% glycerol, and 1 mM DTT. 100-fold molar excess of TCEP (TCEP in buffer of Tris pH 7.4) was added to diluted protein and the container was flushed with N_2 gas. This was incubated for 10 minutes at room temperature. 50 uL of DMF was added to solid dye and this container was mixed and flushed with N_2 gas. Dye was added to protein at 50 uL dye/1 mg protein. Container was flushed with N_2 gas again and mixed gently. This solution was allowed to incubate for 30 minutes at room temperature, and then left on ice for 1.5 hr, mixing gently every 30 minutes. This solution was spun in a series of two Micro Bio-spin columns (Bio-Rad) to remove unincorporated dye, and glycerol was added to the resulting solution to be 10% w/v.

FRET studies

Fluoresecence Resonance Energy Transfer (FRET) studies were performed using a Safire fluorimeter (Tecan), using an excitation wavelength of 550nm and detecting an emission wavelength of 670nm. Experiments were done in a total volume of 20 uL, with 5mM $MgCl_2$, .5 mM nucleotide, and 1 uM of each dye-protein conjugate, in a 500mM NaCl, 25mM Tris pH 8, 10% glycerol buffer at 65°C for ten minutes. Immediately after incubation, samples were transferred to Corning 384 black, flat bottom polystyrene microplates and scanned

5'[^{32}P] oligo labeling

Gel-purified 10mM TP74 (5'-CTGCAGGGTTTTTGTTCCAGTCTGTAGCACTGTGTAAGACAGGCCA-3') were incubated with •-^{32}[P] ATP 32 TP74 and polynucleotide kinase (T4 PNK) in T4 PNK buffer at 37°C for 15 minutes. The unincorporated •-^{32}[P] was removed using a nucleotide removal kit (Quagen). This oligo was then annealed to TP124 (5'CATCTGGCCTGTCTTACACAGTGCTACAGACTGGAACAAAAACCCTGCAG-3') by boiling for 5 minutes followed by slow coiling to 55°C.

Exonuclease reaction

Nuclease assays with annealed oligonucleotides contained 50 nM protein, 25 mM MOPS pH 7.0, 1 mM $MnCl_2$, and 1nM [^{32}P]-labeled oligonucleotide duplex with either DTT or diamide in 10 µl reactions and were incubated at 55°C for 1 hr. Reactions were stopped by adding 0.2% SDS and 10 mM EDTA solution and were analyzed on 20% polyacrylamide denaturing sequencing gels. Gels were exposed on phosphorimager screens and analyzed using a Typhoon phosphorimager (G.E.)

Results

Mutagenesis and Purification of pfRad50-SMA

In this project, the effect of ATP and other nucleotides on Rad50 function and structure was investigated. The structure of pfRad50 shows that binding of a non-hydrolyzable ATP analog stimulates homodimerization by creating a more energetically favorable surface for dimerization. Our strategy involved using artificially introduced cysteine crosslinks so we could observe the effects of linking the ATP-bound, homodimerized form of the protein together to observe functionality. Using the *Pyrococcus furiousus* Rad50 catalytic domain model as determined by X-ray crystallography (Hopfner et al, 2000), residues were mutated to cysteines that were close enough, about 4-6Å, to form disulfide bonds under oxidizing conditions. We made two different crosslinking pairs based on the crystal structure, and as this protein doesn't have any endogenous cysteines, we could be certain that any crosslinking that occurs is coming from these introduced cysteines. The locations of these introduced crosslinks are labeled on the *Pyrococcus furiousus* crystal structure in Figure 1. One of the introduced cysteine pairs was I25C and D864C, which are in positions to link an N- and C- terminal from the same Rad50 molecule. Thus, this pair was called the intradimer crosslink. These residues are located approximately 5.20Å apart from each other, and thus are likely to form a disulfide bond. A second pair, D55C and T790C are approximately 5.95Å and represent the crosslinking of a N- and C-terminal from different Rad50 molecules, and thus was called the interdimer crosslink.

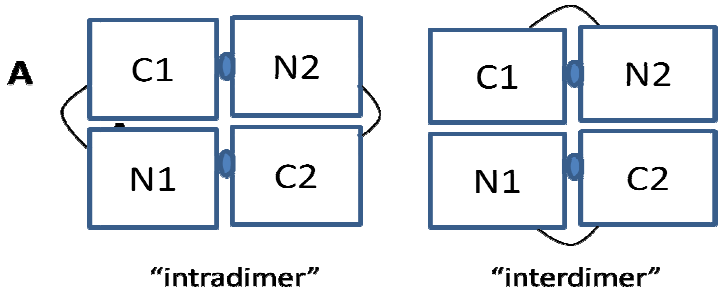

B

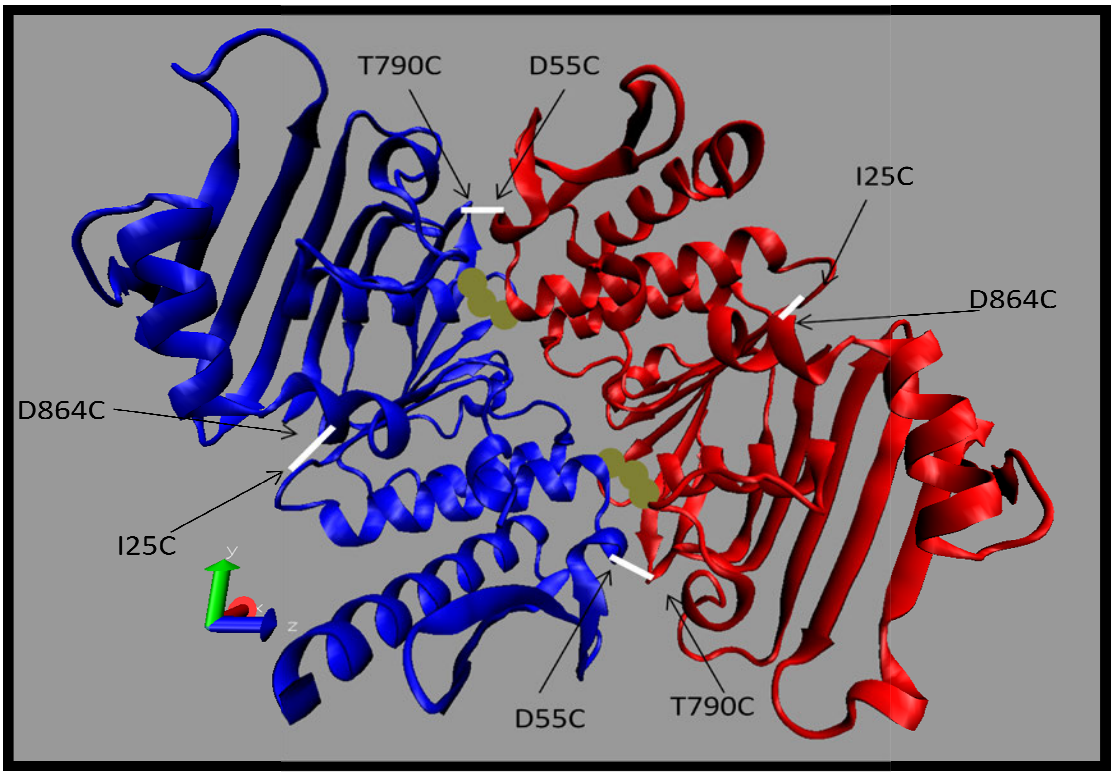

ematic of crystal
green) is bound in
ough here they are
pfner et al. 2000

Quickchange Site-directed mutagenesis (Stratagene) was used to make the proper residue changes in the pfRad50-SMA plasmid. The pfRad50-SMA plasmid has the two Rad50 catalytic domains coexpressed (amino acids 1-149 and 738-883), with a lac operon controlling expression. Added to the C-terminus of the N-terminal Rad50 catalytic domain was a 6x His-tag, which was used for affinity purification. The plasmid was initially transformed into XL10-Gold

Ultracompetent cells as a vector for producing replicating the plasmid. Plasmid was then extracted and purified from XL10-Gold cells and transformed into *E. coli* BL21(DE3) cells, which were used for overexpression of protein.

BL21DE cells with pfRad50-SMA were then grown, induced and harvested for intracellular proteins. The proteins were purified using Ni-affinity chromatography, anion-exchange, and cation-exchange fast protein liquid chromatography (FPLC) as described in Materials and Methods.

The ability to crosslink in the predicted fashion was tested using different reducing/oxidizing conditions and separating species based on size. For separation and visualization of species, SDS-PAGE and Coomassie blue staining was used. SDS-PAGE causes separation of denatured species, but since disulfide bonds are covalent in nature, complexes that have been crosslinked will migrate at a slower rate than a complex that aren't crosslinked. The N-terminal catalytic domain used was approximately 21 kDa and the C-terminal domain was approximately 19.5 kDa. Thus, one would expect to see the two bands around 20 kDa be replaced by a single band around 41 kDa in the case of an intradimer crosslink. When no reducing agent is added to the mixture, a large band appears at about 41 kDa, the size expected for an N- and C-terminal crosslinked (Figure 2).

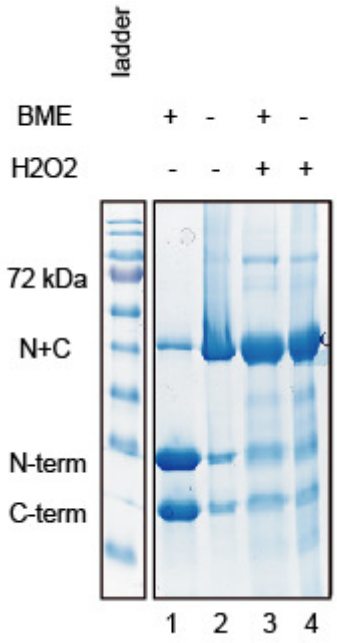

Figure 3: Proof of pfRad50-SMA mer crosslinking. 107 uM pfRad50- w ɔated with 600 mM NaCl for 10 minutes. 25 mM beta-mercaptc l a ci en as i loading buffer as indicated.

Dimerization of Rad50 ca i a y binding. (Hopfner et al, 2000) h , to determine whether the interdimer pfRad50-SMA crosslinked efficiently, reaction med with ATP and Mg^{2+} to stimulate dimeri a ion. Interestingl , ound t 2mM H_2O_2 duri ies appeared on SDS-PAGE. Likely, this was due i n two had been catalyzed. e nds was likely to be a N+N monomer, while the m he lowest C+C. To test this hypothesis, we first com y dimer pfRad50-SMA with.25 m D T nutes on ice. Then, ATP and Mg^{2+} was e ıd the mix was 10 m to catalyze dimerization. Finally, 2mM H_2O_2 vas added to oxidize cysteines in their current i t lly adding DTT

creasing the ratio of the N+C terminal bands ddle band labeled ‘dimer’) to N+N op ba d labeled ‘dimer’) and C+C bands (d labeled ‘dimer’).

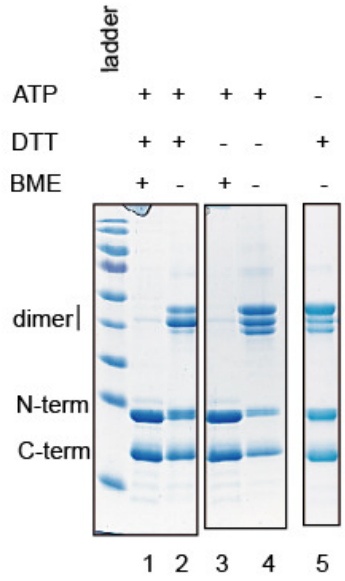

Figure 3: Proof of pfRad50- A mer crosslinking. 83.3 µM pfRad50-S i cu 600mM NaCl, .25 mM DTT for five minutes as indica mM ATP and 5mM $MgCl_2$ d ubated for ten minutes at 65°C. Finally, 2mM H_2O_2 was added and w r i t ce, d act s stopped using SDS loading f M E, as indicated.

y p

steine mutations made to pfRad50 a c t tionality, each s tested for adenylate kinase and ATPase ty. In this assay, with [γ-^{32}P]ATP a ho 65°C, with the levels of P_i generated were used e e s of [β-^{32}P]ADP m ylate kinase activity. comparable to

wild-type protein and the approp c be assumed to

protein.

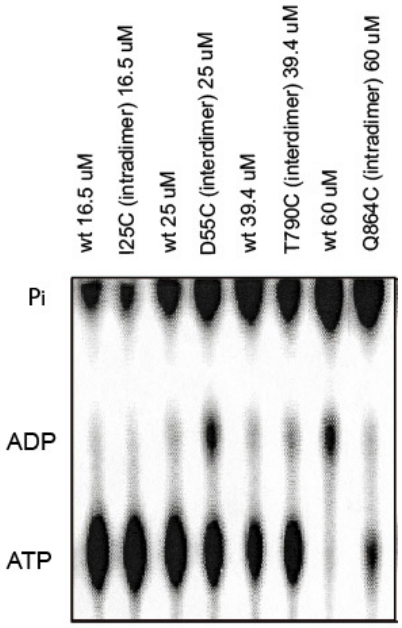

Figure 4 u i ysteine mutants. b te 1 ti n o taining buffer A (20 i H m C ly rol, 1 mM DTT) with 5 mM $MgCl_2$ 5 o D Γ, and 50 µM [γ-^{32}P]ATP. n n n d ed. Reactions were incub te o n e s opped with the addition of 1% SDS and 10 mM EDTA eparated using thin-layer chromatography (TLC).

ociation Constant

, w vestigate the K_d of homodimerization alyzed by ATP. We used SDS- A ofRad50- ncentrations under optimized c tions with ATP. us was determined on i t was obtained by c entration that was run during this experiment w obtained was from 5.5 uM. The SDS-PAGE g d b C Coomassie blue

staining and scanned by a Licor Odyssey machine.

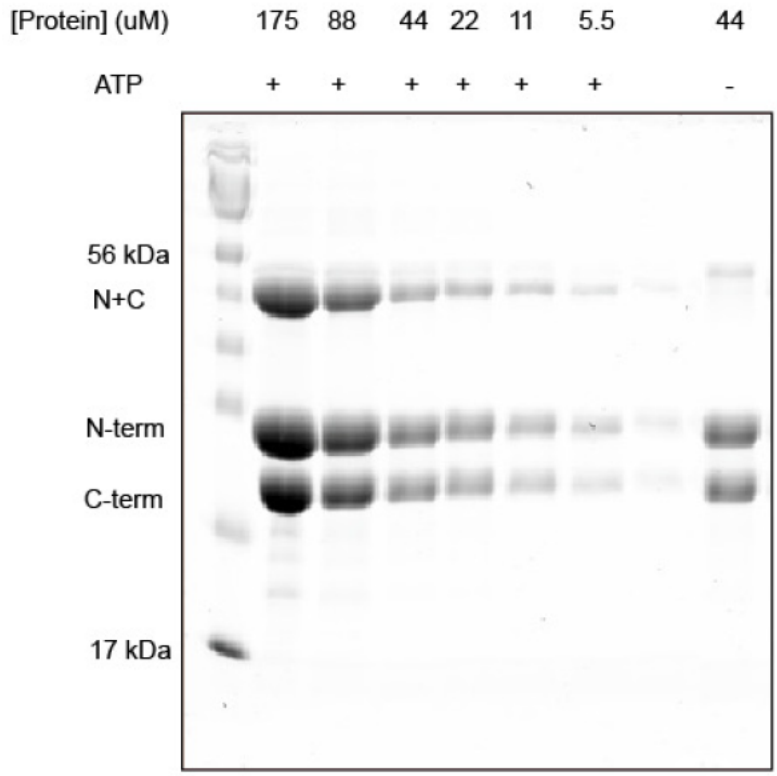

Figure 5: K_d of pfRad50 homodimerization. pfRad50-SMA interdimer in was incubated at 65°C for ten minutes with 5mM $MgCl_2$, .5mM ATP, 25mM MOPS, pH 7.0, 600mM NaCl, and 1mM H_2O_2 at the concentration as indicated.

The images were then quantified using ImageQuant 5.1. The ratio of N+C dimer to total amount of N and C in any form vs. the total concentration of protein was graphed to determine an approximate K_d of homodimerization in Figure 6. It is difficult to determine a definite K_d of homodimerization from the resulting data because of limiting protein concentrations, but it appears that the affinity of the monomers for each other is relatively low (≥100 uM). In the full-length protein the catalytic domains are tethered together through the zinc hook (fig. 1) so a high affinity of association may not be necessary in the context of the full length protein.

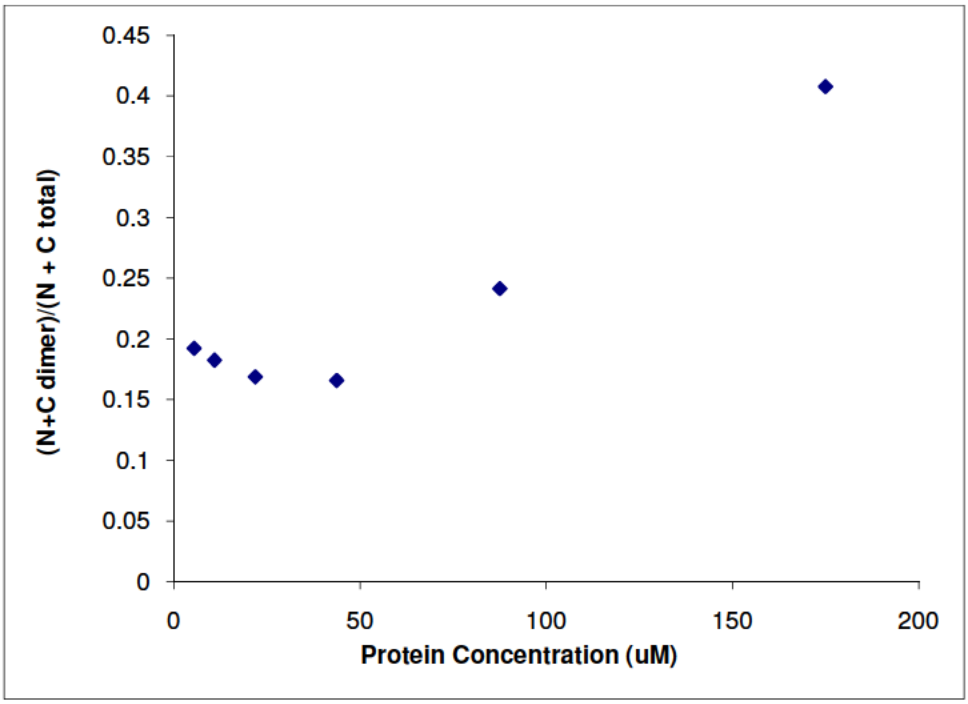

Figure 6: Graph of K_d of pfRad50-SMA homodimerization. The molar ratio of crosslinked dimers to total monomers and dimers vs. concentration of protein incubated was graphed.

Effects of homodimerization on pfRad50-SMA DNA binding

Based on the crystal structure of pfRad50-SMA, it has been hypothesized that homodimerization creates a DNA binding surface on Rad50. As a way to test both the functionality of the protein with the mutations as well as to confirm that dimerization does allow DNA binding, the oxidized interdimer pfRad50-SMA protein was incubated with a 41 base-pair dsDNA that was fluorescently labeled. The reactions in this gel mobility shift assay were separated in a 5.5% native acrylamide gel (Figure 7). The result shows that the protein is still capable of DNA binding, suggesting that homodimerization, at the least, does not abrogate the protein's DNA binding capability.

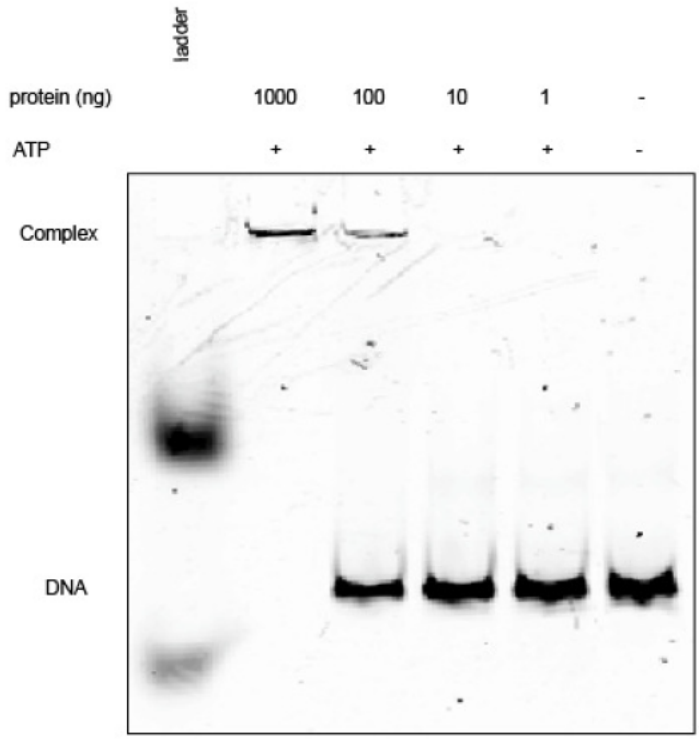

Figure 7: pfRad50-SMA interdimer can bind DNA. pfRad50-SMA interdimer was incubated with 25 mM MOPS pH 7.0, .1 pmol annealed TP2151/TP2109, .5mM ATP, 5mM $MgCl_2$, and 50 mM NaCl, and 1mM H_2O_2, as indicated. Amount of protein in each reaction is indicated. The reactions were separated on a 5.5% acrylamide gel and analyzed using a Typhoon phosphorimager.

Determination of conditions affecting pfRad50 homodimerization using FRET studies

To detect more transient dimerization events, fluorescence resonance energy transfer (FRET) was used. Two mutant pfRad50-SMA proteins, D55C and T790C, were used, which are the same mutations used in the interdimer mutation. Each mutant was purified and a maleimide-fluorescent dye was conjugated to the cysteine residues. Cy3 and Cy5 were the two fluorescent dyes used. The D55C mutant was conjugated to Cy5, while the T790C mutant was conjugated to Cy3. The Cy3/Cy5 fluorescent pair is widely used for energy transfer experiments, as the Cy3 emission wavelength overlaps with the Cy5 excitation wavelength. When the two dyes come in close contact (<50Å) to each other, energy is transferred from an excited Cy3 dye to a Cy5 dye

in a nonradiative manner. The Cy5 dye then emits at a higher wavelength than Cy3 emission. In this manner, one can measure how close two dyes are by exciting with Cy3 wavelength light while simultaneously measuring the Cy5-emission wavelength.

In the FRET experiments here, the two conjugated mutant proteins were mixed and Cy5 emission was measured while being excited at the Cy3 wavelength, under different conditions. In this case, increased signal corresponded to higher percent of homodimerization (Schematic shown in Figure 8) Initially, the effect of different nucleotides was tested (Figure 9). Compared to a no nucleotide control, ATP, with heat and magnesium, significantly increased FRET, and thus decreased the relative distance of the two dyes. Since magnesium is necessary for coordination of the nucleotides, control experiments were performed by not including magnesium. Interestingly, when ADP was present, the average distance of the dyes increased compared to when there was no nucleotide present.

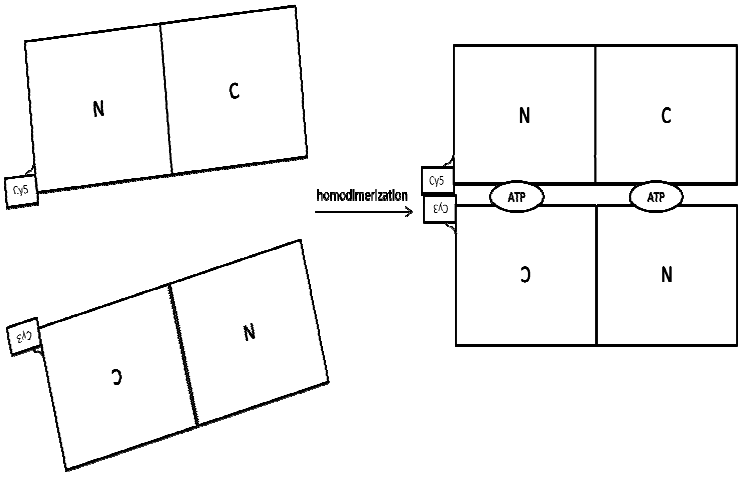

Figure 8: Schematic of FRET assay.

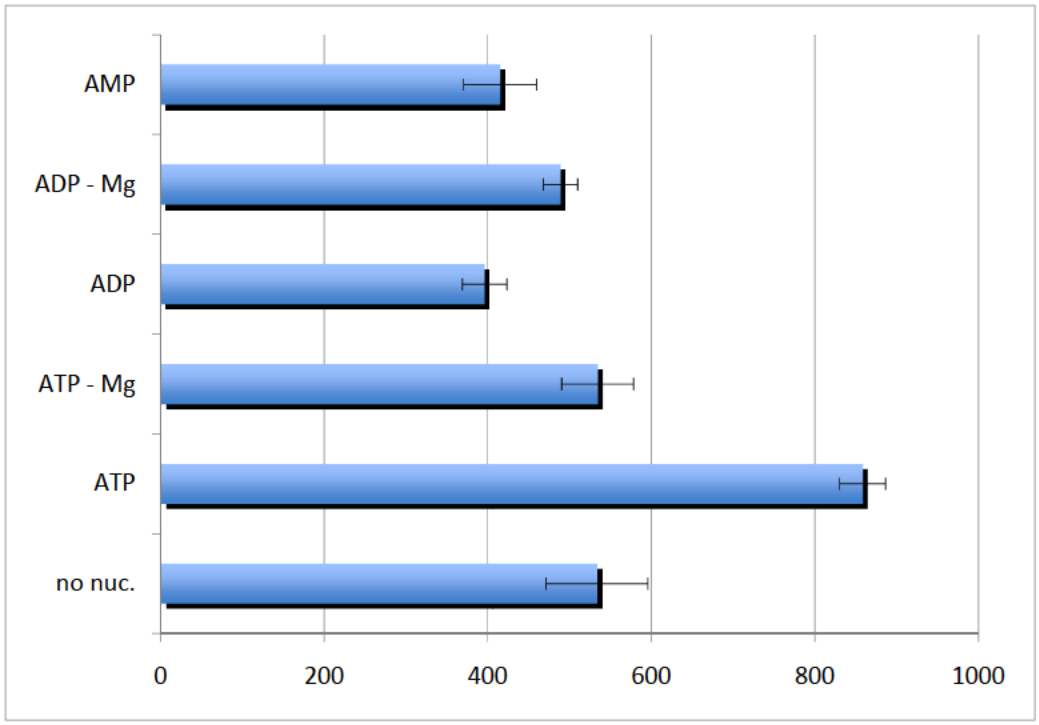

Figure 9: Effect of nucleotides on dimerization of pfRad50-SMA. 1uM Maleimide- Cy5 conjugated D55C pfRad50-SMA and 1μM maleimidie-Cy3 conjugated T790C pfRad50-SMA were incubated with 5mM $MgCl_2$, .5mM nucleotide, and 500mM NaCl, 25mM Tris pH 8.0 at 65°C for ten minutes. These reactions were immediately transferred to a Corning 384-well flat bottom, low volume polystyrene microplate and analyzed using a Safire (Tecan) fluorimeter. Experiments were performed in triplicate, with the error bars being the standard deviation.

We also wanted to determine whether DNA stimulated homodimerization of pfRad50. The FRET system provided a convenient way of testing this. A mixture of the two labeled proteins were incubated with different amounts of a 1kb double-stranded DNA ladder. This included (length of DNA). Both 10ng and 1000ng of dsDNA caused a slight stimulation of homodimerization.

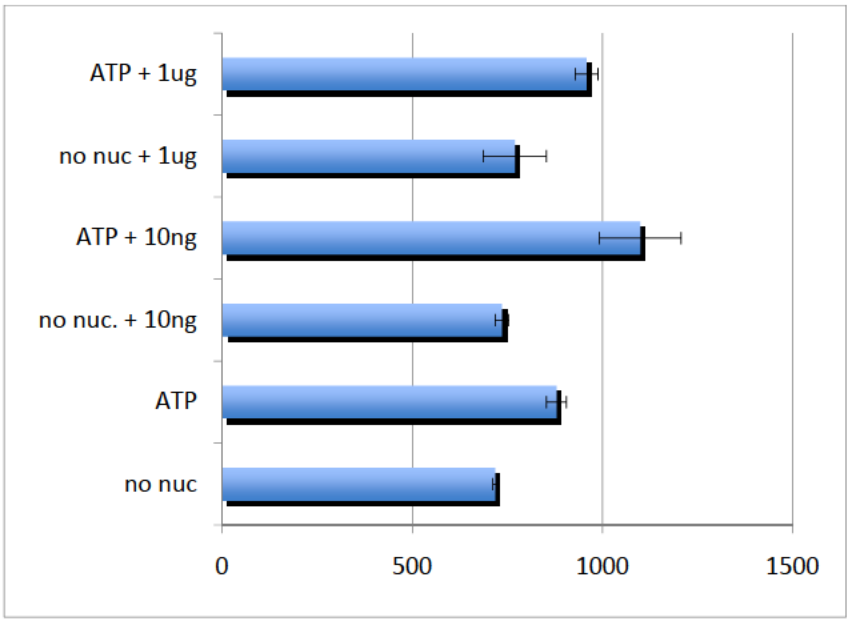

Figure 10: double-stranded DNA shows slight stimulation of homodimerization. 1uM Maleimide- Cy3 conjugated D55C pfRad50-SMA and 1uM maleimide-Cy5 conjugated T790C pfRad50-SMA were incubated with 5mM $MgCl_2$, .5mM ATP, 500mM NaCl, 25mM Tris pH 8.0, and 1kb dsDNA ladder, as indicated, at 65°C for ten minutes. These reactions were immediately transferred to a Corning 384-well flat bottom, low volume polystyrene microplate and analyzed using a Safire (Tecan) fluorimeter. Experiments were performed in triplicate, with the error bars being the standard deviation.

Expression, purification, and crosslinking studies of full length pfMR

The ATP dependent dimerization and DNA binding even with the introduced cysteines indicated that the point mutations themselves didn't affect the structural or functional integrity of pfRad50-SMA. To see what affect dimerization had in a more physiologically relevant system, we made the intradimer and interdimer mutations in the full length pfRad50 that included the coiled-coil domains and zinc-hook. Additionally, now that the coiled-coil was present (which includes the Mre11 binding site), pfMre11 could be coexpressed and the two could form a pfMre11/Rad50 pfMR complex.

Protein expression and purification was performed in a similar manner as done for the pfRad50-SMA. Interestingly, growth of interdimer pfRad50 was significantly retarded compared to the wild-type and intradimer mutant cultures, suggesting toxicity to the expressing cells. To decrease the toxicity to the cells, after induction of protein expression, cells were grown at 24°C for 18 hours instead of the usual 37°C for 4 hours.

The amount of protein was quantified using BSA standards and based on the amount of pfMre11. The concentrations of protein obtained were significantly lower than that of the pfRad50-SMA proteins. Initially, conditions that optimized crosslinking were determined. H_2O_2 was used as an oxidizing agent. 5mM H_2O_2 was determined to be sufficient to cause maximal crosslinking in both the intra- and interdimer mutants. (Figure 11). Theoretically, both inter- and intradimer crosslinks should produce circular products. Though the molecular weight of the intradimer crosslinker wouldn't change upon crosslinking, the circular formation would likely cause a retardation of movement through an acrylamide gel, as was observed.

The interdimer mutant's homodimerization should be ATP-dependent. Interestingly, two bands at around the size of full length pfRad50 were observed. Under oxidizing conditions, the lower band that is expected for pfRad50 began to disappear in an ATP-dependent fashion. Additionally, it was observed that the pfMre11 band disappeared in coordination with the pfRad50 band. Though no significant amount of larger band was observed, it is likely that a higher order structure could not have been observed using the staining technique used or that the complex was stuck in the well.

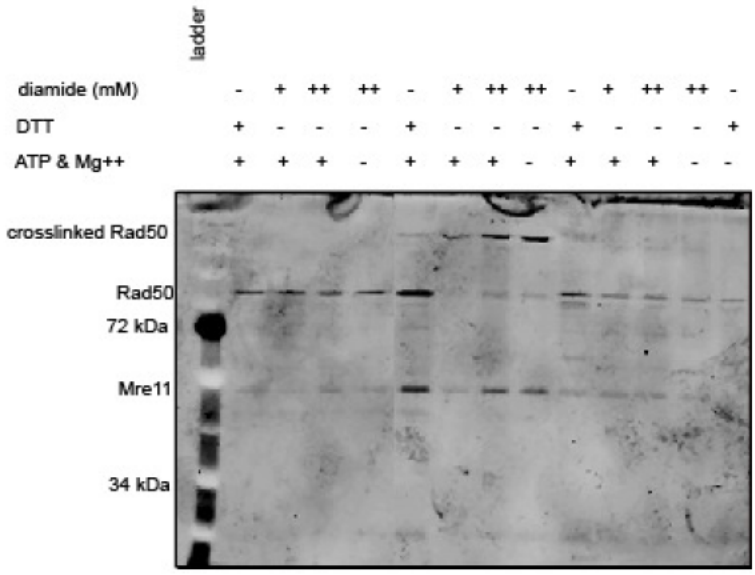

Figure 11: Effect of oxidizing agent on pfMR interdimer. 180nM pfMR intradimer or 200nM pfMR interdimer was incubated with 500mM NaCl, H_2O_2, 5mM $MgCl_2$, .5 mM ATP, 5mM DTT, 150nM or 300 nM diamide as indicated. Additionally, 25mM BME was added to the loading dye as indicated, and run on a 6% acrylamide gel.

Effects of homodimerization on pfMR 3' exonuclease activity

The pfMR complex has been shown to exhibit 3' to 5' exonuclease activity in the presence of manganese that is dependent on both Mre11 and Rad50 catalytic activities.[15] To determine whether this activity was abrogated by Rad50 dimerization, the exonuclease activity of the complex was tested in crosslinking conditions and non-crosslinking conditions. A [^{32}P] 5' labeled dsDNA with a 3' overhang, as is shown in the schematic in Figure 12A, was used to test the exonuclease activity of the complex under different conditions. As this activity was shown to be ATP- and manganese-dependent, .5mM ATP and 1mM $MnCl_2$ were added.

Hydrogen peroxide causes nonspecific DNA degradation. To circumvent this, diamide was used as the oxidizing agent in the exonuclease assay, as it is specific to crosslink sulfur to form thiol bonds and wouldn't itself affect DNA stability. At a diamide concentration of 150nM,

at which the intra- and interdimer mutants would be effectively crosslinked, the wild type and intradimer complex's exonuclease activity of the complex were not affected; however, the exonuclease of the interdimer complex was significantly abrogated. This suggests that either Rad50 needs to be a monomer for proper exonuclease function of the complex or that a conformational change, which is inhibited by Rad50 interdimer crosslinking, is needed for proper exonuclease function.

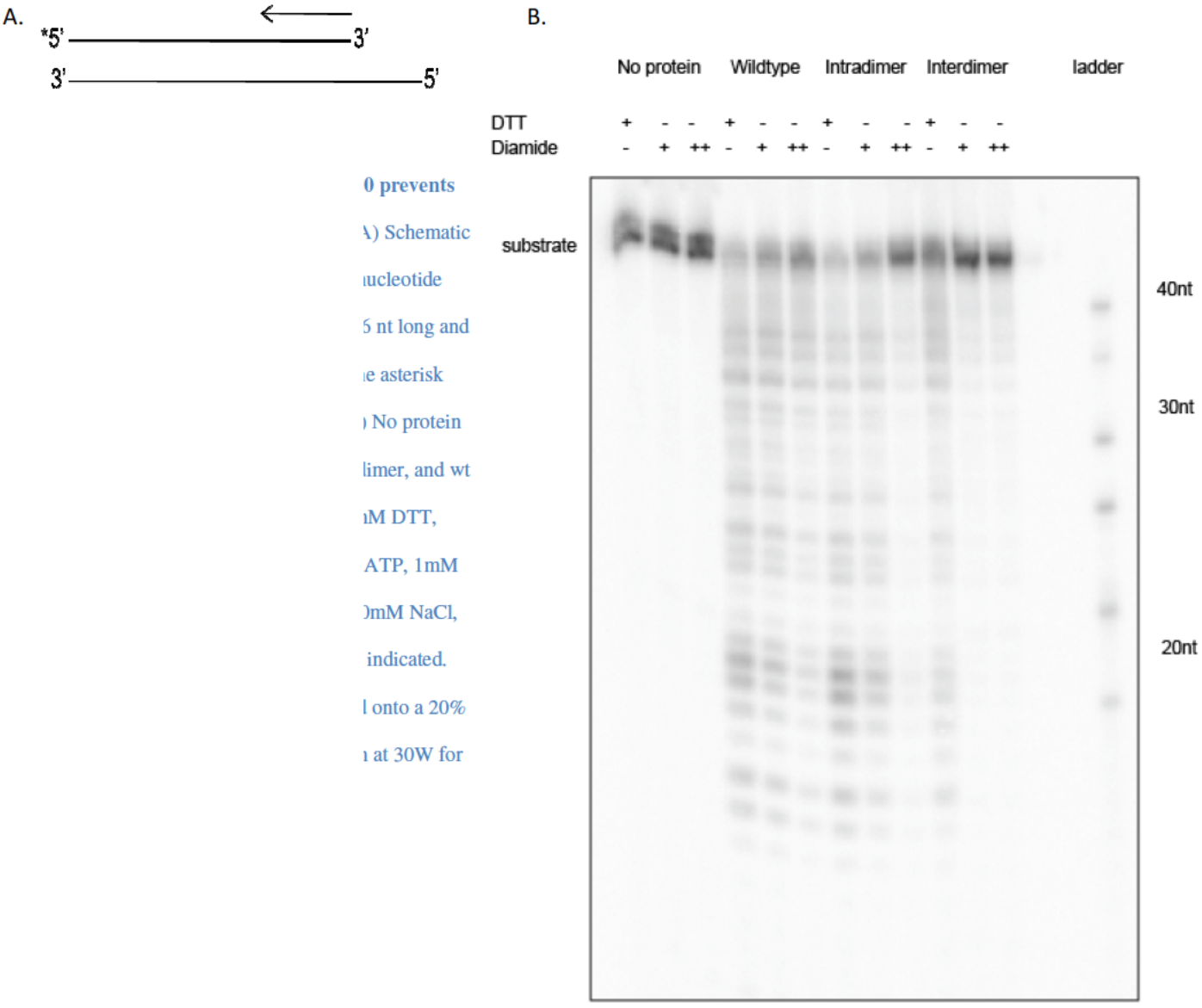

0 prevents

A) Schematic

ucleotide

5 nt long and

e asterisk

) No protein

limer, and wt

M DTT,

ATP, 1mM

)mM NaCl,

indicated.

l onto a 20%

ı at 30W for

Discussion

In the work presented here, using site-directed crosslinking I show that the homodimerized catalytic domains of pfRad50 can bind DNA. Furthermore, using fluorescently tagged pfRad50, I showed that homodimerization of the catalytic domains is stimulated by ATP and slightly inhibited by ADP. Additionally, homodimerization of these domains is slightly stimulated by the presence of double-stranded DNA. Finally, I show that the manganese-dependent exonuclease activity present in full length pfMR is strongly inhibited by the locking of the pfRad50 into a homodimerized state.

Using SDS-PAGE, intradimer crosslinking between pfRad50-SMA was confirmed. The efficient crosslinking of the separate catalytic domains in oxidizing conditions confirms that the X-ray crystal structure of pfRad50 catalytic domains is physiologically relevant. (Hopfner et al, 2000) The three bands that appeared at the size of a double N-terminal crosslink, a double C-terminal crosslink, and a N+C crosslink suggests that without ATP there is no affinity to homodimerize. The largest of the three bands, the double N terminal crosslink, had the highest population without the presence of ATP, suggesting that the design of these cysteine replacements were most accessible to spontaneous thiol formation.

Using the interdimer pfRad50-SMA mutant incubated at various concentrations, the resulting species were analyzed to try to determine the dissociation constant of homodimerization of pfRad50. At concentrations below 44μM, the ratio between homodimers and monomers became constant. As the ratio should continue to fall as the concentration is lowered, it is likely that the Colloidal Coomassie Blue staining and Odyssey Imager doesn't provide a high enough resolution. In the future, running the homodimerization reactions again at

a titration of concentrations, but using a more sensitive staining method, such as Krypton staining, can potentially overcome this.

Based on structural information of the pfRad50 catalytic domains, homodimerization has been speculated to create a DNA binding cleft on the surface of the dimer. The gel-shift DNA binding assay performed here supports this hypothesis, as even pfRad50 that is locked into a homodimerized state shows the ability to bind DNA. However, from this data, it is hard to definitely say that the DNA binding activity is due to the fraction of the mutant that is dimerized or the fraction that isn't dimerized. To provide more rigorous evidence that the dimerized state of Rad50 is able to bind DNA, an additional DNA binding experiment wherein wild-type pfRad50-SMA was run at the same concentrations and under the same conditions as the homodimerized pfRad50-SMA could be performed. If homodimerization does form a DNA binding cleft, one would expect an increased amount of DNA-protein complex for the covalently homodimerized complex compared to the wild-type complex.

Full length intradimer and interdimer Rad50 pfMR complex were expressed and purified, and this complex was tested for its ability to crosslink. The intradimer complex worked as expected, showing a larger band when run under crosslinking conditions in an acrylamide gel. This crosslinked product is expected to be the same molecular weight as the noncrosslinked species, but should form a circular product as opposed to a linear, noncrosslinked species, which would have retarded movement through an acrylamide gel.

The interdimer crosslinking results were not as clear. Though the interdimer pfRad50 band did show an ATP- and oxidized-dependent disappearance, as is expected, this also coincided with the disappearance of the pfMre11 band. A hardly visible band was seen to appear

at the very top of the gel, which is likely the resulting complex. The fact that Mre11 disappeared suggests that there is some kind of very stable interaction between Mre11 and Rad50. A convenient explanation would have been the disappearance of Mre11 due to endogenously located cysteines in Mre11 crosslinking one of the two introduced cysteines in the interdimer mutant. However, there are no endogenous cysteines located in pfMre11. Mre11 is thought to bind to Rad50 even in the monomeric form, and thus the dimerization would likely be creating a conformational change that greatly enhances the complexs interactions, so much so that they would be resistant to denaturation by SDS. This hypothesis could be tested further by obtaining sequences of both the Mre11, Rad50 and the hardly visible band that appears at the top of the gel using N-terminal sequencing. Additionally, a structure of the pfMR complex is currently being obtained in other labratories, which may prove useful for determining the nature of this phenomena.

To test the effects of Rad50 homodimerization on the functionality of the pfMR complex, we tested the complex's manganese-dependent 3' exonuclease activity. This activity is thought to be facilitated initially by the postulated weak, ATP-dependent unwinding of a DNA end by Rad50. Then, Mre11 can degrade DNA from the opened 3' end. The homodimerized complex showed significantly decreased exonuclease activity compared to its reduced form. Likely, the unwinding activity of Rad50 requires not only ATP binding but ATP hydrolysis. The interdimer linking of Rad50 would not allow hydrolysis due to restriction of conformational changes (including dimer dissociation). In this way, unwinding wouldn't occur and the exonuclease activity would be inhibited, as is shown in Figure 12. Though this presents a compelling argument, more work must be done to determine the exact conformational change, whether dimer dissociation or otherwise, that is necessary for DNA unwinding in pfRad50.

The ability of nucleotides to induce homodimerization was tested using Fluorescence resonance energy transfer between fluorophores attached to cysteines near the homodimerization interface. As expected, ATP produced a strong signal for homodimerization. It has been suggested that there is an ADP binding site separate from that of the ATP pocket on Rad50. Interestingly, when ADP is added instead of ATP, a slight decrease in the distance between the two fluorophores was observed, suggesting that ADP may actually decrease the chance of homodimerization compared to when there is no nucleotide present at all. Since even with no nucleotide, there is a likely a small amount of Rad50 molecules that dimerize, it is plausible that the ADP-bound Rad50 is not capable of forming even a fraction of homodimers. To become more confident in the data, however, one should run this experiment over again with more replicates.

Finally, the effect of DNA on ATP-induced pfRad50 homodimerization was determined. As there is a proposed dsDNA double-stranded binding site on pfRad50, we used our FRET assay to determine whether dsDNA increased the amount of homodimerized catalytic domains. Along with standard homodimerization conditions, the addition of both 10ng and 1000ng of 1kb DNA ladder showed slight stimulation of homodimerization. This suggests that either DNA somehow increases the affinity for the two monomers to each other, or that it binds after homodimerization has already occurred and acts to stabilize the homodimer. Because there is a titration of sizes of nucleotides in the ladder, one could determine whether one size contributes the most significantly to homodimerization stimulation by running this experiment with only a single size of dsDNA.

This series of experiments has many important implications towards the structure and mechanism of Rad50 and Mre11. First, the X-ray crystal model obtained by Hopfner *et al*, 2000

has been shown to be physiologically relevant. Additionally, ADP has been shown to slightly inhibit homodimerization, suggesting a model where pfRad50 is in two significantly different conformations depending on whether ATP or ADP is bound. DNA also stimulated a slight affinity for pfRad50 homodimerization, suggesting its ability to stabilize Rad50 in its dimer form. Finally, the exonuclease activity of the full length pfMR complex has been shown to be abrogated by forced homodimers, suggesting that some kind of significant conformational change is needed for exonuclease activity – likely Rad50's DNA unwinding ability. This data opens up many questions as to the mechanism and role of Rad50 homodimerization.

References

Ajimura, M., Leem, S.H., and Ogawa, H. (1993). Identification of new genes required for meiotic recombination in *Saccharomyces cerevisiae*. Genetics *133*, 51-66.

Alani, E., Padmore, R., and Kleckner, N. (1990). Analysis of wild-type and rad50 mutants of yeast suggests an intimate relationship between meiotic chromosome synapsis and recombination. Cell *61*, 419-436.

Aravind, L., Walker, D.R., and Koonin, E.V. (1999). Conserved domains in DNA repair proteins and evolution of repair systems. Nucleic Acids Res *27*, 1223-1242.

Bakkenist, C.J., and Kastan, M.B. (2003). DNA damage activates ATM through intermolecular autophosphorylation and dimer dissociation. Nature *421*, 499-506.

Bhaskara, V., Dupre, A., Lengsfeld, B., Hopkins, B.B., Chan, A., Lee, J.H., Zhang, X., Gautier, J., Zakian, V.A., and Paull, T.T. (2007). Rad50 Adenylate Kinase Activity Regulates DNA Tethering by Mre11/Rad50 complexes. Molecular Cell *25*, 647-661.

Blinov, V.M., Koonin, E.V., Gorbalenya, A.E., Kaliman, A.V., and Kryukov, V.M. (1989). Two early genes of bacteriophage T5 encode proteins containing an NTP-binding sequence motif and probably involved in DNA replication, recombination and repair. FEBS Lett *252*, 47-52.

Carney, J.P., Maser, R.S., Olivares, H., Davis, E.M., Le Beau, M., Yates, J.R., 3rd, Hays, L., Morgan, W.F., and Petrini, J.H. (1998). The hMre11/hRad50 protein complex and Nijmegen breakage syndrome: linkage of double-strand break repair to the cellular DNA damage response. Cell *93*, 477-486.

Chamankhah, M., Fontanie, T., and Xiao, W. (2000). The Saccharomyces cerevisiae mre11(ts) allele confers a separation of DNA repair and telomere maintenance functions. Genetics *155*, 569-576.

Chen, C., and Kolodner, R.D. (1999). Gross chromosomal rearrangements in Saccharomyces cerevisiae replication and recombination defective mutants. Nat Genet *23*, 81-85.

de Jager, M., van Noort, J., van Gent, D.C., Dekker, C., Kanaar, R., and Wyman, C. (2001). Human Rad50/Mre11 is a flexible complex that can tether DNA ends. Mol Cell *8*, 1129-1135.

de Jager, M., Wyman, C., van Gent, D.C., and Kanaar, R. (2002). DNA end-binding specificity of human Rad50/Mre11 is influenced by ATP. Nucleic Acids Res *30*, 4425-4431.

Gellert, M. (2002). V(D)J recombination: RAG proteins, repair factors, and regulation. Annu Rev Biochem *71*, 101-132.

Goldberg, M., Stucki, M., Falck, J., D'Amours, D., Rahman, D., Pappin, D., Bartek, J., and Jackson, S.P. (2003). MDC1 is required for the intra-S-phase DNA damage checkpoint. Nature *421*, 952-956.

Gorbalenya, A.E., and Koonin, E.V. (1990). Superfamily of UvrA-related NTP-binding proteins. Implications for rational classification of recombination/repair systems. J Mol Biol *213*, 583-591.

Hopfner, K.P., Karcher, A., Craig, L., Woo, T.T., Carney, J.P., and Tainer, J.A. (2001). Structural biochemistry and interaction architecture of the DNA double-strand break repair Mre11 nuclease and Rad50-ATPase. Cell *105*, 473-485.

Hopfner, K.P., Karcher, A., Shin, D.S., Craig, L., Arthur, L.M., Carney, J.P., and Tainer, J.A. (2000). Structural biology of Rad50 ATPase: ATP-driven conformational control in DNA double-strand break repair and the ABC-ATPase superfamily. Cell *101*, 789-800.

Hopfner, K.P. (2006). The Mre11/Rad50/Nbs1 Complex. In DNA Damage Recognition, W. Siede, ed. (New York, New York: Taylor and Francis) pp.705-721.

Ivanov, E.L., Korolev, V.G., and Fabre, F. (1992). XRS2, a DNA repair gene of *Saccharomyces cerevisiae*, is needed for meiotic recombination. Genetics *132*, 651-664.

Johzuka, K., and Ogawa, H. (1995). Interaction of Mre11 and Rad50: two proteins required for DNA repair and meiosis-specific double-strand break formation in *Saccharomyces cerevisiae*. Genetics *139*, 1521-1532.

Karagiannis, T.C., and El-Osta, A. (2004). Double-strand breaks: signaling pathways and repair mechanisms. Cell Mol Life Sci *61*, 2137-2147.

Kaye, J.A., Melo, J.A., Cheung, S.K., Vaze, M.B., Haber, J.E., and Toczyski, D.P. (2004). DNA breaks promote genomic instability by impeding proper chromosome segregation. Curr Biol *14*, 2096-2106.

Klein, I., Sarkadi, B., and Varadi, A. (1999). An inventory of the human ABC proteins. Biochim Biophys Acta *1461*, 237-262.

Kupiec, M., and Simchen, G. (1984). Cloning and mapping of the RAD50 gene of Saccharomyces cerevisiae. Mol Gen Genet *193*, 525-531.

Lewis, L.K., and Resnick, M.A. (2000). Tying up loose ends: nonhomologous end-joining in Saccharomyces cerevisiae. Mutat Res *451*, 71-89.

Linton, K.J., and Higgins, C.F. (1998). The Escherichia coli ATP-binding cassette (ABC) proteins. Mol Microbiol *28*, 5-13.

Lobachev, K.S., Gordenin, D.A., and Resnick, M.A. (2002). The Mre11 complex is required for repair of hairpin-capped double-strand breaks and prevention of chromosome rearrangements. Cell *108*, 183-193.

Lukas, C., Melander, F., Stucki, M., Falck, J., Bekker-Jensen, S., Goldberg, M., Lerenthal, Y., Jackson S. P., Bartek, J., Lukas, J. (2004). Mdc1 couples DNA double-strand break recognition with its H2Ax-dependent chromatin retention. EMBO J. *23*, 2674-2683.

Maser, R.S., Mirzoeva, O.K., Wells, J., Olivares, H., Williams, B.R., Zinkel, R.A., Farnham, P.J., and Petrini, J.H. (2001). Mre11 complex and DNA replication: linkage to E2F and sites of DNA synthesis. Mol Cell Biol *21*, 6006-6016.

Mirzoeva, O.K., and Petrini, J.H. (2003). DNA replication-dependent nuclear dynamics of the Mre11 complex. Mol Cancer Res *1*, 207-218.

Moreau, S., Ferguson, J.R., and Symington, L.S. (1999). The nuclease activity of Mre11 is required for meiosis but not for mating type switching, end joining, or telomere maintenance. Mol Cell Biol *19*, 556-566.

Paull, T.T., and Gellert, M. (1998). The 3' to 5' exonuclease activity of Mre 11 facilitates repair of DNA double-strand breaks. Mol Cell *1*, 969-979.

Shiloh, Y. (2003). ATM and related protein kinases: safeguarding genome integrity. Nat Rev Cancer *3*, 155-168.

Stewart, G.S., Maser, R.S., Stankovic, T., Bressan, D.A., Kaplan, M.I., Jaspers, N.G., Raams, A., Byrd, P.J., Petrini, J.H., and Taylor, A.M. (1999). The DNA double-strand break repair gene *hMre11* is mutated in individuals with an Ataxia-Telangiectasia-like disorder. Cell *99*, 577-587.

Stewart, G.S., Wang, B., Bignell, C.R., Taylor, A.M., and Elledge, S.J. (2003). MDC1 is a mediator of the mammalian DNA damage checkpoint. Nature *421*, 961-966.

Takata, M., Sasaki, M.S., Sonoda, E., Morrison, C., Hashimoto, M., Utsumi, H., Yamaguchi-Iwai, Y., Shinohara, A., and Takeda, S. (1998). Homologous recombination and non-homologous end-joining

pathways of DNA double-strand break repair have overlapping roles in the maintenance of chromosomal integrity in vertebrate cells. EMBO J *17*, 5497-5508.

Trujillo, K.M., and Sung, P. (2001). DNA structure-specific nuclease activities in the Saccharomyces cerevisiae Rad50/Mre11 complex. J Biol Chem *13*, 13.

Weterings, E., and van Gent, D.C. (2004). The mechanism of non-homologous end-joining: a synopsis of synapsis. DNA Repair (Amst) *3*, 1425-1435.

Zhang, X., and Paull, T.T. (2005). The Mre11/Rad50/Xrs2 complex and non-homologous end-joining of incompatible ends in S. cerevisiae. DNA Repair (Amst) *4*, 1281-1294.

Acknowledgements

I would like to thank Dr. Tanya Paull for her guidance and mentorship and allowing me to work independently in the lab. Her assistance has been invaluable in my maturing as a scientist. I also owe thanks to Dr. Rajashree Deshpande and Ben Hopkins, who have taught me the techniques I have used in this project. Furthermore, I am indebted to the entire Paull Lab, who provided tremendous encouragement and help during my time in lab. Additionally, I owe thanks to Dr. Adrian Keatinge-Clay for his helpful comments on this manuscript.

Finally, I would like to thank my friends for their encouragement, and my family for their endless support, without both I wouldn't have had such a terrific past four years.

This work was funded in part by the American Society for Microbiology Undergraduate Research Fellowship and the University of Texas Undergraduate Research Fellowship.